

Equation of state from weak shocks in solids

Duane C. Wallace

Los Alamos Scientific Laboratory, Los Alamos, New Mexico 87545

(Received 17 April 1979)

The Rankine-Hugoniot jump conditions for the increases across a shock of the normal stress, normal strain, and internal energy are not valid for weak shocks in solids. Correct jump equations for a solid can be obtained by integrating the equations for conservation of mass, momentum, and energy along the Rayleigh line through the shock process; these jump equations then depend on the details of the shock profile. Further, because a uniaxially compressed solid supports a nonzero shear stress, the locus of thermodynamic states reached behind planar shocks, which we call the anisotropic Hugoniot, requires for its description two stress variables and two strain variables. In the present paper the thermodynamic description of the anisotropic Hugoniot is given, and for the example of 6061-T6 Al the shock-profile jump equations are derived, the weak-shock equation of state is computed, and the pressure on the principal adiabat is found to differ from the results of Rankine-Hugoniot theory by several percent in the range 0–100 kbar.

I. INTRODUCTION

Shock experiments have been extensively used to determine equations of state of solids.¹⁻⁴ The quantities measured are the shock and particle velocities, and from these the Hugoniot equation of state, a pressure-volume-energy curve, is computed by means of the Rankine-Hugoniot jump conditions. Since these jump conditions were constructed specifically to describe shocks in gases or liquids,⁵⁻⁷ their use to analyze shocks in solids represents the neglect of differences in solid and liquid behavior. This situation has been recognized in the past,¹⁻⁴ but the theory and the experimental data needed to correct for solid-liquid differences were not available. In the present paper we present the needed theory for the case of weak planar shocks in initially isotropic solids.

It is helpful at the outset to identify the characteristics of shocks in solids which are to be accounted for in this work. The Rankine-Hugoniot jump conditions and related thermodynamic analyses⁵⁻⁷ will be referred to as "liquid Hugoniot theory." This theory assumes that the shock is a single steady wave, which means the jump conditions can be calculated by the black box treatment: The entire shock front is considered a black box of fixed thickness which moves at the shock speed; ahead of the box is material in the initial equilibrium state and behind the box is uniformly moving material in the final equilibrium state. Without knowing any details of the shock structure it is still possible to apply conservation laws: Whatever flows into the box must flow out. In this way conservation of mass, momentum, and energy give relations among the following three quantities: the normal strain from initial to final state, the corresponding change

in the normal stress, and the change in the internal energy. Since these are thermodynamic quantities, by the assumption of initial and final equilibrium, it is then possible to calculate the increase in entropy through the shock, a very appealing result of the theory. Unfortunately, however, the black-box treatment does not work for a weak shock in a solid. For since the elastic precursor travels faster than the plastic wave, the entire shock front is not a steady wave; it spreads continuously and takes in an ever increasing mass of material, and momentum and energy. This means the shock is a sink for these quantities, and the steady Rankine-Hugoniot jump conditions across the shock do not hold: All of what flows in does not flow out. Conservation of mass, momentum, and energy still hold on the local scale, but the total change in these quantities across the shock will depend on the spreading of the shock profile.

The other approximation of liquid Hugoniot theory is that the material behind the shock is in a state of isotropic pressure. This means there is only one stress variable and one strain variable on the Hugoniot, namely the pressure and the volume, and the liquid jump conditions are sufficient to specify these uniquely. A solid, however, after uniaxial compression by a planar shock, presumably supports a nonzero shear stress, so the final state is characterized by two stress variables and two strain variables; jump conditions on the normal stress and the normal strain are insufficient to determine all four of these stress and strain variables.

In Sec. II we set up a thermodynamic description of the anisotropic (tetragonal) Hugoniot for a solid; this description is not limited to weak shocks. In Sec. III we show how the weak-shock Hugoniot can be constructed from shock profiles,

and carry out the construction for 6061-T6 Al. Once the anisotropic Hugoniot is determined, it is possible to calculate isotropic pressure curves, including the principal adiabat; the theory for this is also derived in Sec. III, and the adiabat for 6061-T6 Al is compared with the corresponding curve calculated from liquid Hugoniot theory.

II. ANISOTROPIC HUGONIOT THERMODYNAMICS

The term Hugoniot will be used here to mean the sequence of thermodynamic equilibrium states reached behind each shock for a sequence of different-strength shocks from a given initial state. Our first job is to specify the Hugoniot in terms of thermodynamic variables. Since they are equilibrium states, they may be reached by a thermoelastic (reversible) process from the initial state. For an initially isotropic solid in plane-shock geometry, the stress and configuration variables are shown in Fig. 1. Cartesian coordinate 1 is the normal (propagation) direction and coordinates 2 and 3 are equivalent transverse directions. An element of mass in the initial configuration has dimensions $d_a, w_a,$ and density $\rho_a,$ and zero applied stress; in the final configuration it has dimensions $d, w,$ density $\rho,$ and normal compressive stress σ and transverse compressive stress $\sigma - 2\tau.$ The final shear stress is $\tau.$ The configuration transformation from initial to final state is given by the elastic transformation matrix $\underline{\alpha}^e,$ ^{8,9} whose elements for the simple transformation of Fig. 1 are (Voigt notation)

$$\begin{aligned} \alpha_1^e &= d/d_a, & \alpha_2^e &= \alpha_3^e = w/w_a, \\ \alpha_4^e &= \alpha_5^e = \alpha_6^e = 0. \end{aligned} \tag{1}$$

The conservation of mass equation for $\underline{\alpha}^e$ is⁸

$$\rho_a/\rho = V/V_a = \det \underline{\alpha}^e = \alpha_1^e \alpha_2^e \alpha_3^e, \tag{2}$$

where $V = \rho^{-1}$ is the volume per unit mass. As shown in Fig. 1, there is also an increase in the entropy, from S_a in the initial state to S in the final state.

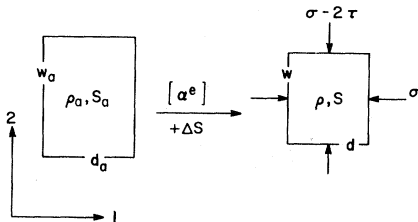


FIG. 1. Thermoelastic transformation of a mass element from the initial state to a final state which is on the anisotropic Hugoniot.

There is a different process by which the material can be brought from the same initial to final states shown in Fig. 1. This is the dynamic (irreversible) process which occurs during planar shock compression.^{9,10} It is characterized by simultaneous elastic strain $\underline{\alpha}^e$ and plastic flow $\underline{\alpha}^p,$ so there are four strain variables, but with the restrictions that the total transverse strain is zero and the plastic flow is volume conserving, there are only two independent strain variables, which can be taken as the total normal strain ϵ and the plastic strain $\psi:$

$$\epsilon = 1 - V/V_a, \tag{3}$$

$$\psi = -\ln \alpha_1^p. \tag{4}$$

The elastic strains are then related to ϵ and ψ by

$$\alpha_1^e = (1 - \epsilon)e^\psi, \tag{5}$$

$$\alpha_2^e = e^{-\psi/2}. \tag{6}$$

For the moment, however, let us forget about shocks. We consider the Hugoniot to be an equilibrium thermodynamic curve of states reached through anisotropic elastic compression by a tetragonal stress system, while some reversible heat $dQ = TdS$ is put in from an external source. For stress-strain variables on the Hugoniot we take the set $\sigma, \tau, \alpha_1^e, \alpha_2^e,$ or what is equivalent through Eqs. 2 and 3, σ, τ, V or $\epsilon, \alpha_2^e.$ Then we proceed to find relations between these and other thermodynamic functions. Note the use of the variable V does not imply that the compression is isotropic or that the stress system is isotropic. Also note that there is no plastic flow on the Hugoniot; nevertheless the material must be presumed to be hardened in some way, so as to support elastically the shear stress $\tau.$ This point will be examined at the end of this section.

The thermodynamics of elastically anisotropic materials is well described in textbooks.^{8,11} For the geometry of Fig. 1, the combined first and second laws are

$$TdS = dU + \sigma dV - 4V\tau d \ln \alpha_2^e, \tag{7}$$

where U is the internal energy per unit mass, S is the entropy per unit mass, and T is the temperature. An independent equation for dS is the identity which results from considering T as a function of S and the elastic strains,

$$TdS = C_\eta dT + TC_\eta [\gamma_1 d \ln V - 2(\gamma_1 - \gamma_2) d \ln \alpha_2^e], \tag{8}$$

where C_η is the heat capacity at constant elastic configuration and γ_1, γ_2 are the anisotropic Grüneisen parameters (Voigt indices, see Ref. 9 or 11 for definitions). Between Eqs. (7) and (8), T and S can be calculated by integrating up the Hugoniot if the other quantities are known on the

Hugoniot. The entropy is small in weak shocks, but not as small as in liquid Hugoniot theory. In particular, because σ and τ are of lowest-order linear in strains [Eqs. (9) and (10) below], the lowest-order terms in (7) and (8) are of second order, and these terms do not cancel in $\int dS$, so $S - S_a$ on the Hugoniot is of second order in strains. In liquid Hugoniot theory,⁵⁻⁷ because $\tau = 0$ on the Hugoniot, the second-order terms cancel and $S - S_a$ is of order ϵ^3 at small ϵ .

Another useful set of equations results from considering σ and τ as functions of S and the elastic strains, and calculating variations:

$$d\sigma = \rho\gamma_1 T dS - B_{11} d \ln V + 2(B_{11} - B_{12}) d \ln \alpha_2^e, \quad (9)$$

$$d\tau = \frac{1}{2}\rho(\gamma_1 - \gamma_2) T dS - \frac{1}{2}(B_{11} - B_{21}) d \ln V + (B_{11} + \frac{1}{2}B_{22} + \frac{1}{2}B_{23} - B_{12} - B_{21}) d \ln \alpha_2^e, \quad (10)$$

$$B_{11} = \lambda + 2\mu - (4\lambda + 8\mu + 2\xi + 4\xi)\epsilon - (8\lambda + 20\mu + 8\xi)\ln \alpha_2^e, \quad (12)$$

$$B_{11} - B_{12} = 2\mu - (4\lambda + 10\mu + 4\xi)\epsilon - (6\lambda + 24\mu + 6\xi + \nu)\ln \alpha_2^e, \quad (13)$$

$$B_{11} - B_{21} = 2\mu - (4\lambda + 8\mu + 4\xi)\epsilon - (6\lambda + 18\mu + 6\xi + \nu)\ln \alpha_2^e, \quad (14)$$

$$B_{11} + \frac{1}{2}B_{22} + \frac{1}{2}B_{23} - B_{12} - B_{21} = 3\mu - (3\lambda + 9\mu + 3\xi + \frac{1}{2}\nu)\epsilon - (18\mu + 3\nu)\ln \alpha_2^e. \quad (15)$$

Equations (12)–(15) are correct to first order in strains at constant entropy; they are also correct to first order in strains in the region of the Hugoniot, because entropy contributions are formally of second order there.

We can now clarify the point of work hardening on the Hugoniot. The Hugoniot described by Eqs. (7)–(10) is entirely thermoelastic; the elastic strains are presumed homogeneous (or at least slowly varying on an atomic scale), and the energy stored in these strains is recoverably by reducing the stresses to zero. In the conservation of energy, Eq. (7), no energy has been allotted to work hardening. However, when a real solid is shocked to the Hugoniot, a small amount of energy is used to accomplish the work hardening and remains stored in the defect structure of the solid. Such energy is elastic in nature, inhomogeneous on an atomic scale, and recoverable by annealing; it does not correspond to the same stress-strain relation, or any other thermoelastic relation, as does the energy stored in homogeneous elastic strain. Now in our dynamic theory of the shock process, the energy associated with work hardening is accounted for through conservation of energy, but it is not stored in any “recoverable” form; it is instead assigned as part of the dissipation. Hence if we use the dynamic theory and shock data to calculate the thermodynamic variables in the shock-compressed state, we construct a Hugoniot which is the same as the one described by Eqs. (7)–(10) and which approximates the real

where $B_{\beta\gamma}$ are the adiabatic stress-strain coefficients. Equations (9) and (10) hold everywhere for the configuration change of Fig. 1, i.e., they hold for arbitrary strains and entropy, or for arbitrary stresses and entropy. For the present tetragonal geometry, two of the $B_{\beta\gamma}$ are related by

$$B_{21} = B_{12} - 2\tau. \quad (11)$$

If enough were known of the quantities on the Hugoniot, Eqs. (9) and (10) could be used to find information about the $B_{\beta\gamma}$ coefficients; this is analogous to the calculation of the bulk modulus in liquid Hugoniot theory.³

In the small strain region the $B_{\beta\gamma}$ can be expanded at constant S in terms of the two adiabatic second-order elastic constants λ , μ and the three adiabatic third-order elastic constants ξ , ξ , ν , as⁸

physical Hugoniot by replacing energy stored in the defect structure by heat. The error is small, as discussed in Ref. 9.

III. THE SHOCK EQUATION OF STATE

A. Construction of the Hugoniot

We proceed now specifically for the case of 6061-T6 Al and base our calculations on the profile measurements of Johnson and Barker¹² and on the methods previously developed for analyzing them.¹⁰ The experimental profiles are described by three regions on the graph of particle velocity v as a function of time (Fig. 2):

- (1) The front from state a to state b is the elas-

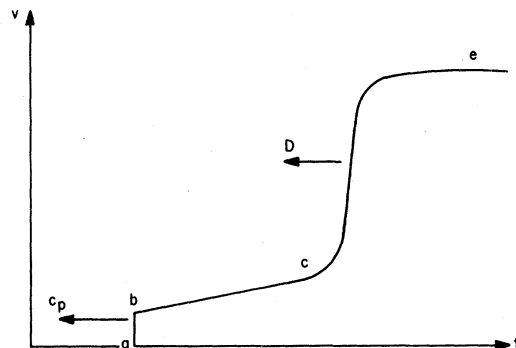


FIG. 2. Schematic representation of a shock moving as two steady waves and an intervening unsteady region. Particle velocity v as a function of time t .

tic precursor, a steady wave moving at velocity c_p ; $v_b = \text{constant}$.

(2) The plastic precursor is an unsteady region from state b to state c ; $v_c = \text{constant}$.

(3) The plastic wave extends from state c to the final Hugoniot state e , is steady, and moves at velocity D .

The experimental profile data needed here are

$$\begin{aligned} v_a &= \epsilon_a = \sigma_a = 0, \\ v_b &= 0.0236 \text{ mm}/\mu\text{s}, \quad v_c = 0.050 \text{ mm}/\mu\text{s}, \\ c_p &= 6.46 \text{ mm}/\mu\text{s}, \\ D &= 5.26 + 1.47v_e \text{ mm}/\mu\text{s}. \end{aligned} \quad (16)$$

The jump conditions for ϵ , σ , U are obtained by integrating the conservation equations through the profile with the following results.¹⁰

At b :

$$\begin{aligned} \epsilon_b &= v_b/c_p, \\ \sigma_b &= \rho_a c_p v_b, \\ U_b - U_a &= \frac{1}{2} c_p^2 \epsilon_b^2. \end{aligned} \quad (17)$$

At c :

$$\begin{aligned} \epsilon_c &= c_p^{-1} v_c + \frac{1}{2} c_p^{-1} (v_c - v_b) \delta, \\ \sigma_c &= \rho_a c_p v_c - \frac{1}{2} \rho_a c_p (v_c - v_b) \delta + \dots, \\ U_c - U_a &= \frac{1}{2} c_p^2 \epsilon_c^2 - \frac{1}{3} D c_p (\epsilon_c - \epsilon_b)^2 \delta + \dots. \end{aligned} \quad (18)$$

At e :

$$\begin{aligned} \epsilon_e &= \epsilon_c + D^{-1} (v_e - v_c), \\ \sigma_e &= \sigma_c + \rho_a D (v_e - v_c), \\ U_e - U_a &= \frac{1}{2} D^2 (\epsilon_e^2 - \epsilon_c^2) + \frac{1}{2} c_p^2 \epsilon_c^2 \\ &\quad + D c_p [(\epsilon_c + \epsilon_b)(\epsilon_e - \epsilon_c) \\ &\quad - \frac{1}{3} (\epsilon_c - \epsilon_b)^2] \delta + \dots. \end{aligned} \quad (19)$$

The small quantity δ ($\delta \ll 1$) is

$$\delta = (c_p - D)/D, \quad (20)$$

and in (18) and (19) the \dots represent terms of second and higher order in δ which arise from

a series expansion of $\sigma(v)$ in the unsteady region from state b to state c . The expansion was made to facilitate analytic integration of the internal energy $dU = V_a \sigma d\epsilon$. The final-state particle velocity v_e may be eliminated from Eqs. (19) in favor of the shock velocity D by the experimental relation (16). The shock velocity is not defined for $v_e < v_c$.

Equations (17)–(19) constitute the jump conditions for ϵ , σ , U , from the initial state a to the final Hugoniot state e . Final-state values for 6061-T6 Al up to $\sigma \approx 100$ kbar are listed in Table I.

The equations for the shear stress τ and the plastic strain ψ through the profile are the same as Eqs. (9) and (10), with TdS replaced by the dynamic entropy production $2V\tau d\psi$ and with $d \ln \alpha_2^e$ replaced by $-\frac{1}{2} d\psi$ according to (6). It is not possible in principle to find jump conditions for τ and ψ because the equations for them at state e contain $\int_a^e \tau d\psi$, the integral to be evaluated along the path of the process. In practice this problem can be eliminated by constructing an approximate jump condition for the integral itself. We expect the integral to be roughly proportional to ϵ_e^2 , since $S_e - S_a$ is of second order in strains. For 6061-T6 Al the integral was evaluated numerically in Ref. 10 for six shock profiles ranging from 21 to 89 kbar; a check of these integrations shows

$$\int_a^e \tau d\psi = (32 \pm 3) \epsilon_e^2, \quad (21)$$

(in kbar) for all the profiles. We therefore calculated τ and $\ln \alpha_2^e = -\frac{1}{2} \psi$ on the Hugoniot, from integrals of Eqs. (9) and (10) with the expansions (12)–(15) for the $B_{\beta\gamma}$ coefficients, the resulting equations being the same as (18) and (19) of Ref. 10. We also used the function $32\epsilon_e^2$ kbar as an interpolation approximation for the integral (21) and the experimental elastic constants of Clifton.¹³

TABLE I. The anisotropic Hugoniot for 6061-T6 Al in the weak-shock region.

ϵ	D (mm/ μ s)	σ (kbar)	$U - U_a$ (10^9 erg/g)	$-\ln \alpha_2^e$	τ (kbar)	T (K)	$S - S_a$ (10^5 erg/g K)	$S - S_a$ (Liquid theory)
0		0	0	0	0	295	0	0
0.0037 ^a		4.1	0.003	0	1.1	297	0	0
0.0082 ^b	5.3335	8.2	0.013	0.0009	1.6	300	0.07	0.003
0.020	5.364	17.7	0.072	0.0049	1.7	310	0.4	0.04
0.040	5.596	35.4	0.274	0.0117	1.8	326	1.2	0.31
0.060	5.775	55.4	0.63	0.0183	2.2	345	2.4	1.1
0.080	5.966	77.9	1.17	0.0247	3.1	368	4.3	2.7
0.100	6.169	103.4	1.92	0.0305	4.7	398	7.4	5.4

^a Corresponds to profile point b .

^b Corresponds to profile point c .

The results are listed in Table I.

With the energy and the stresses and strains known, it is possible to integrate Eqs. (7) and (8) up the Hugoniot to find T and S . The thermodynamic coefficients in these equations were evaluated by a set of approximations whose justification was discussed in the profile analysis,¹⁰ and which are of sufficient accuracy here as well:

$$\gamma_1 = \gamma_2 = \gamma, \quad \rho\gamma = \rho_a\gamma_a, \quad \gamma_a = 2.16, \quad (22)$$

$$C_\eta = C_V = 0.88 \times 10^7 \text{ erg/g K}.$$

Values of temperature and entropy on the Hugoniot are also listed in Table I.

B. Construction of isotropic pressure curves

The next problem is the following: Given σ , τ , α_1^e , α_2^e on the Hugoniot, construct a P - V curve. This can be done in different ways by carrying out a thermoelastic strain from the anisotropic Hugoniot to conditions of isotropic pressure. We could, for example, hold σ constant and increase the transverse compressive stress until it equals σ , adiabatically. An alternate process, which we use here because of its simplicity in plane-wave geometry, is to bring the shear stress to zero under conditions of constant density and entropy. The thermoelastic process is described by equations of the preceding section, in particular (7)–(10), specialized to $dV = 0$ and $dS = 0$:

$$dU = 4Vd \ln \alpha_2^e, \quad (23)$$

$$dT = 2T(\gamma_1 - \gamma_2)d \ln \alpha_2^e, \quad (24)$$

$$d\sigma = 2(B_{11} - B_{12})d \ln \alpha_2^e, \quad (25)$$

$$d\tau = bd \ln \alpha_2^e, \quad (26)$$

where b is the combination

$$b = B_{11} + \frac{1}{2}B_{22} + \frac{1}{2}B_{23} - B_{12} - B_{21}. \quad (27)$$

For abbreviation, the P - V curve to be constructed will be called the isotrope. Equations (23)–(26) are to be integrated from a point on the Hugoniot (denoted by subscript H) to the corresponding point on the isotrope (denoted by subscript I). The independent variable of the integration is τ , which goes from τ_H to 0; Eq. (26) may be used to eliminate $d \ln \alpha_2^e$ in favor of $d\tau$ in (23)–(25). Since the integration ranges are small increments (the isotrope is close to the Hugoniot), the $B_{\beta\gamma}$ are taken constant for each integral. To integrate dT , the approximations (22) for the anisotropic Grüneisen parameters are used, which implies $dT = 0$. The isotrope may then be calculated from the Hugoniot by the equations

$$S_I = S_H, \quad (28)$$

$$V_I = V_H, \quad (29)$$

$$U_I = U_H - 2(V/b)\tau_H^2, \quad (30)$$

$$T_I = T_H, \quad (31)$$

$$P_I = \sigma_H - 2[(B_{11} - B_{12})/b]\tau_H. \quad (32)$$

The difference $\sigma_H - P_I$ at a common value of V and S is approximately $\frac{4}{3}\tau_H$; Eqs. (12)–(15) can be used to make a small-strain expansion of (32) to find

$$\begin{aligned} \sigma_H - P_I &= \frac{4}{3}\tau_H \left[1 - \mu^{-1}(\lambda + 2\mu + \xi - \frac{1}{6}\nu) \right. \\ &\quad \left. \times (\epsilon + 3 \ln \alpha_{2H}^e) + \dots \right] \\ &= \frac{4}{3}\tau_H \left[1 - \mu^{-1}(\lambda + 2\mu + \xi - \frac{1}{6}\nu) \right. \\ &\quad \left. \times (\tau_H/\mu) + \dots \right]. \quad (33) \end{aligned}$$

The term of order τ_H/μ should usually be quite small.

To evaluate the isotrope for 6061-T6 Al, we used the expressions (12)–(15) for the $B_{\beta\gamma}$ and the elastic-constant data of Clifton.¹³ This constitutes a neglect of contributions to the $B_{\beta\gamma}$ from the entropy on the Hugoniot and from fourth-order elastic constants. The thermodynamic functions so calculated are listed in Table II. Regarding the principal elastic strains α_1^e and α_2^e , we have available two equations from which they may be evaluated on the isotrope: the integral of Eq. (26),

$$\ln(\alpha_{2H}^e/\alpha_{2I}^e) = b^{-1}\tau_H, \quad (34)$$

and Eq. (2) for conservation of mass,

$$\ln \rho_I/\rho_a = -\ln \alpha_{1I}^e - 2 \ln \alpha_{2I}^e. \quad (35)$$

However, as there is only one stress measure to the isotrope, namely P_I , there is for an isotropic material only one strain measure, say V_I or ρ_I , and it is not necessary to evaluate α_1^e and α_2^e . In other words, α_1^e and α_2^e become equal on the isotrope, and (34) and (35) are not independent.¹⁴ The change in the material configuration in going from the Hugoniot to the isotrope is

TABLE II. The isotrope and the principal adiabat for 6061-T6 Al.

ρ (g/cm ³)	Isotrope		Adiabat	
	P (kbar)	T (K)	P (kbar)	T (K)
2.703	0	295	0	295
2.713	2.7	297	2.7	297
2.725	6.1	300	6.1	300
2.758	15.5	310	15.4	308
2.816	32.9	326	32.7	322
2.876	52.4	345	51.9	336
2.938	73.7	368	72.8	351
3.003	97.0	398	95.4	366

shown in Fig. 3.

It is now straightforward to calculate the principal adiabat, which is the pressure-volume curve at constant entropy $S = S_a$. A convenient process for going from isotope to adiabat is to reduce S from S_I to S_a at constant V by extracting reversible heat from the material. Ordinary P - V thermodynamics gives¹¹

$$dU = TdS - PdV, \quad (36)$$

$$TdS = C_V dT + \rho\gamma C_V T dV, \quad (37)$$

$$\rho\gamma = \left(\frac{\partial P}{\partial U} \right)_V. \quad (38)$$

From these equations, the differentials at constant V are

$$dU = TdS = C_V dT = (\rho\gamma)^{-1} dP. \quad (39)$$

In going from the isotope to the adiabat, the independent integration variable is S . Again since the integration ranges are small increments, the coefficients C_V and $\rho\gamma$ can be set constant for each integral. The adiabat, denoted by subscript A , may then be calculated from the isotope by the equations

$$S_A = S_a, \quad (40)$$

$$V_A = V_I, \quad (41)$$

$$T_A = T_I \exp[-(S_I - S_a)/C_V], \quad (42)$$

$$P_A = P_I + \rho\gamma C_V (T_A - T_I), \quad (43)$$

$$U_A = U_I + C_V (T_A - T_I). \quad (44)$$

The principal adiabat for 6061-T6 Al is listed in Table II. The stresses on the anisotropic Hugoniot and the pressure on the isotope and the

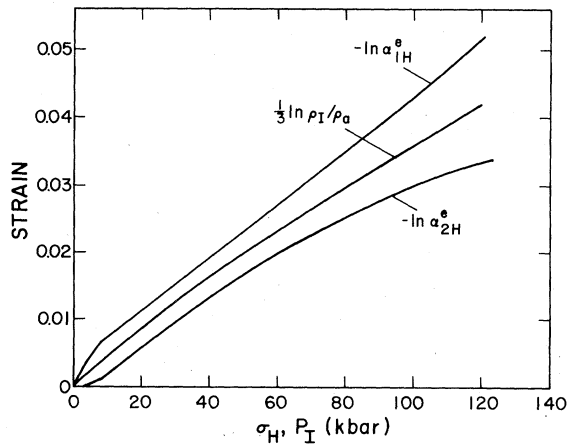


FIG. 3. Change in the elastic-strain variables in going from the anisotropic Hugoniot to the isotropic pressure curve. The density ρ_I on the isotope is related to the elastic strains on the isotope by Eq. (35).

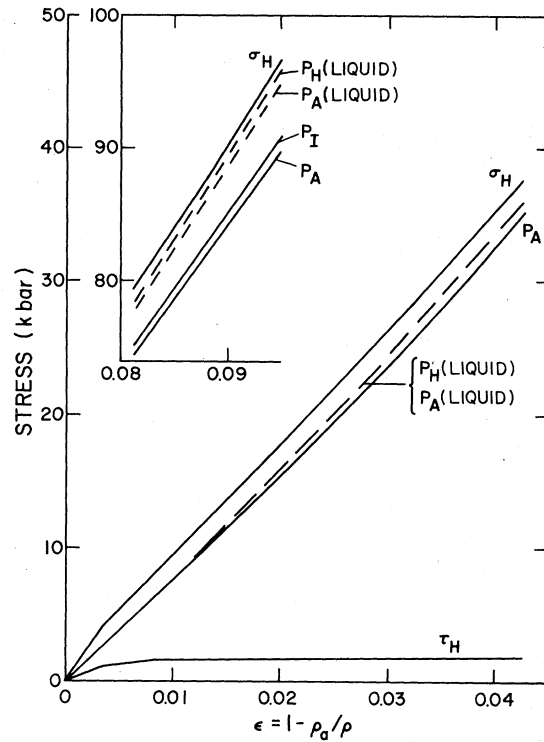


FIG. 4. Stresses as a function of elastic strain: σ_H and τ_H are on the anisotropic Hugoniot, P_I is on the isotope, and P_A is on the principal adiabat, and representing liquid Hugoniot theory, P_H (liquid) is on the Hugoniot and P_A (liquid) is on the principal adiabat.

adiabat, as functions of the compression, are compared graphically in Fig. 4.

C. Approximate P - V curves

Having carried out an accurate calculation of the weak-shock equation of state for 6061-T6 Al, it is interesting to calculate the same property by means of liquid Hugoniot theory based on the same experimental data. The difference of liquid Hugoniot theory⁵⁻⁷ from the present anisotropic Hugoniot theory can be made clear in two separate steps.

(1) Liquid Hugoniot theory says the elastic and plastic precursors do not exist; jump conditions for a single steady wave then follow. These jump conditions may be obtained as a special case of Eqs. (19) by eliminating the elastic and plastic precursors, i.e., by setting $v_b = v_c = 0$:

$$\begin{aligned} \epsilon_e &= D^{-1} v_e, \\ \sigma_e &= \rho_a D v_e, \\ U_e - U_a &= \frac{1}{2} D^2 \epsilon_e^2. \end{aligned} \quad (45)$$

(2) Liquid Hugoniot theory then says $\tau_e = 0$, which means the Eqs. (45) determine an isotropic pres-

sure curve with

$$\sigma_e = P_e. \quad (46)$$

When the shock velocity is a linear function of the final-state particle velocity, the above equations of liquid Hugoniot theory simplify to³

$$\begin{aligned} D &= c + s v_e, \\ P_e &= \rho_a c^2 \epsilon_e (1 - s \epsilon_e)^{-2}, \\ U_e - U_a &= \frac{1}{2} V_a P_e \epsilon_e. \end{aligned} \quad (47)$$

We used the experimental shock-velocity-particle-velocity relation (16) to calculate the pressure and energy as functions of compression on the liquid Hugoniot for 6061-T6 Al. We also calculated T and S on the liquid Hugoniot by integrating Eqs. (7) and (8) and then constructed the principal adiabat by means of Eqs. (40)–(44), all using the same approximations (22) for γ and C_V as before. The liquid results are compared with results of the anisotropic theory in Fig. 4.

A well-known approximation for the P - V curve is due to Murnaghan¹⁵; this is simply a first-order Maclaurin expansion in pressure for the bulk modulus and we will apply it here for the adiabatic bulk modulus on the line of constant entropy:

$$B(P, S_a) = B_0 + B'_0 P, \quad (48)$$

where B is the adiabatic bulk modulus, B_0 is B at $P=0$ and $S=S_a$, and B'_0 is $(\partial B/\partial P)_S$ at $P=0$ and $S=S_a$. Equation (48) integrates to the Murnaghan form for $P(V)$ in the present case along the principal adiabat,

$$P(V, S_a) = \frac{B_0}{B'_0} \left[\left(\frac{V_a}{V} \right)^{B'_0} - 1 \right]. \quad (49)$$

For 6061-T6 Al at room temperature and zero pressure, Clifton's¹³ measurements give

$$\begin{aligned} B_0 &= 728 \text{ kbar}, \\ B'_0 &= 5.275. \end{aligned} \quad (50)$$

The differences from our accurate adiabat of the Murnaghan approximation and of the adiabat constructed from liquid Hugoniot theory are shown in Fig. 5, in the form of ΔP_A at a fixed volume, defined by

$$\Delta P_A = \frac{P_A(V)_{\text{approx}} - P_A(V)}{P_A(V)}. \quad (51)$$

D. Errors

On the Hugoniot, the relations $\sigma(\epsilon)$ and $U(\epsilon) - U_a$ are determined entirely from shock-profile data, through the profile jump equations (17)–(19), and these relations as listed in Table I should be quite accurate, σ to within 1% and $U - U_a$ to 2%. The

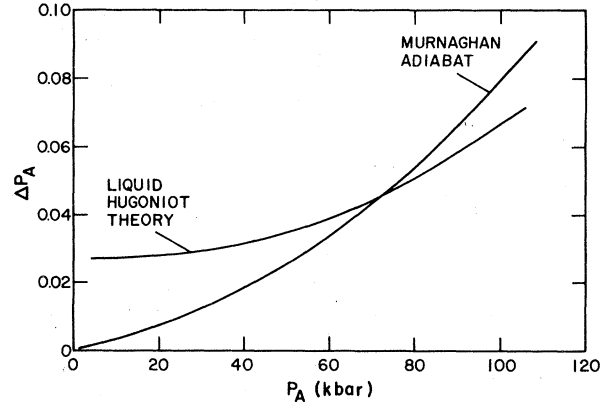


FIG. 5. Relative difference ΔP_A in the pressure P_A on the principal adiabat for two approximations as compared with the accurate calculations of the present paper. ΔP_A is defined by Eq. (51).

main source of error is expected to be the shock-velocity-particle-velocity data. The error most significant in specifying the Hugoniot, and in determining the isotrope and the adiabat, is the error in τ . This arises mainly from errors in the $\sigma(\epsilon)$ relation and in the $B_{B\gamma}$ coefficients. We have not attempted to estimate the fourth-order-elastic-constant contributions to $B_{B\gamma}$; it is hard to imagine, however, that the τ values listed in Table I can be in error by more than 25% up to 50 kbar and by more than 50% up to 100 kbar. The error in $S=S_a$ on the Hugoniot comes from our approximations for γ and C_V and from evaluation of the profile integral $\int_a^e \tau d\psi$. The latter is determined with good precision, say of order 10%, independently of larger errors in τ in the final state. $S - S_a$ should be accurate to within 20% on the Hugoniot.

In transforming from the Hugoniot to the isotrope, the process is approximately equivalent to replacing the stress system σ, τ at each density and entropy by a pressure $P_I \approx \sigma - \frac{4}{3}\tau$. Hence the error in P on the isotrope is essentially the sum of the errors in σ and τ on the Hugoniot. Finally in going to the adiabat, the pressure change $P_A - P_I$ will be in error by about the same percentage as is $S_H - S_a$, giving an error in P_A by at most a few tenths kbar at 100 kbar. All in all the pressure on the adiabat, Table II, should be accurate to 1 kbar at 50 kbar and to about 4 kbar at 100 kbar.

The error in liquid Hugoniot theory can be estimated with more precision, by comparing its results with those of the anisotropic Hugoniot theory, because the same shock-velocity-particle-velocity relation was used in both calculations, and the same approximations for γ and C_V

as well. There are two differences between the two theories: The anisotropic Hugoniot has non-zero τ (the major effect) and it has a slightly larger entropy than the liquid Hugoniot. The role of these two effects is easily seen at the point where the shock velocity is equal to the elastic precursor velocity because here the ϵ , σ , U jump conditions are the same for both theories [compare Eqs. (17)–(19) with (45) for the case $D=c_p$]. At this value of ϵ , then, σ is equal for the two Hugoniot curves, at about 143 kbar for 6061-T6 Al. Integrating out the shear stress from the anisotropic Hugoniot, say at constant ϵ , reduces the pressure by about $\frac{1}{3}\tau$ below the liquid Hugoniot. Integrating out the entropy from either curve to reach the adiabat also reduces the pressure, but more so in the case of the anisotropic Hugoniot because it has the higher entropy. Both effects work in the same direction, although in the present aluminum calculations the entropy effect is only about 5% of the $\frac{1}{3}\tau$ effect. These comments, and our numerical results, are summarized as follows:

(a) For shocks in the neighborhood of $D=c_p$, liquid Hugoniot theory produces a pressure which is too high by about $\frac{1}{3}\tau$.

(b) For the 6061-T6 Al adiabat from 0 to 100 kbar, liquid Hugoniot theory produces a pressure which is too high by several percent (Fig. 5).

The Murnaghan adiabat (49) was evaluated entirely from elastic constant data, Eq. (50). In the

low-pressure region this represents the most reliable determination of the $P_A(V)$ curve. It is gratifying to find that the anisotropic Hugoniot, which is mainly determined by shock data, gives a $P_A(V)$, after integrating out the sizable shear stress, in agreement with the Murnaghan curve in the low-pressure region.

E. Stronger shocks

The relative error in using liquid Hugoniot theory for solids depends primarily on the value of τ/σ on the anisotropic Hugoniot. In the present analysis this ratio is roughly constant in the range 50–100 kbar, but it is reasonable to expect it eventually to decrease as a function of shock strength, and hence to expect liquid Hugoniot theory to become more accurate for stronger shocks.

IV. CONCLUSIONS

A method for extracting true thermodynamic information from a wave-profile analysis has been illustrated with data on 6061-T6 Al. In addition to obtaining proper thermodynamic variables of the material undergoing fast one-dimensional deformation, an equation of state for the material can be measured at stresses intermediate between the low values obtained in static experiments and the higher values in shock experiments where strength corrections presumably become smaller.

¹J. M. Walsh, M. H. Rice, R. G. McQueen, and F. L. Yarger, *Phys. Rev.* **108**, 196 (1957).

²L. V. Al'tshuler, *Usp. Fiz. Nauk* **85**, 197 (1965) [*Sov. Phys. Usp.* **8**, 52 (1965)].

³R. G. McQueen, S. P. Marsh, J. W. Taylor, J. N. Fritz, and W. J. Carter, in *High Velocity Impact Phenomena*, edited by R. Kinslow (Academic, New York, 1970), p. 293.

⁴J. A. Morgan, *High Temp.—High Pressures* **6**, 195 (1974); **7**, 65 (1975).

⁵R. Courant and K. O. Friedrichs, *Supersonic Flow and Shock Waves* (Interscience, New York, 1948).

⁶L. D. Landau and E. M. Lifshitz, *Fluid Mechanics* (Pergamon, London, 1959).

⁷Ya. B. Zel'dovich and Yu. P. Raizer, *Physics of Shock Waves and High-Temperature Hydrodynamic Phenomena* (Academic, New York, 1966), Vol. 1.

⁸D. C. Wallace, in *Solid State Physics*, edited by H. Ehrenreich, F. Seitz, and D. Turnbull (Academic, New York, 1970), Vol. 25, p. 301.

⁹D. C. Wallace, this issue, *Phys. Rev. B* **22**, 1477

(1980).

¹⁰D. C. Wallace, preceding paper, *Phys. Rev. B* **22**, 1487 (1980).

¹¹D. C. Wallace, *Thermodynamics of Crystals* (Wiley, New York, 1972).

¹²J. N. Johnson and L. M. Barker, *J. Appl. Phys.* **40**, 4321 (1969).

¹³R. J. Clifton, in *Shock Waves and the Mechanical Properties of Solids*, edited by J. J. Burke and V. Weiss (Syracuse University Press, Syracuse, 1971), p. 73.

¹⁴The two principal elastic strains α_1^0 and α_2^0 would not be equal on the isotrope for a single crystal of symmetry lower than cubic, or for an anisotropically prepared polycrystal (e.g., cold rolled); hence for any real material after shock compression there will be a small effect of this nature due to the anisotropic working of the shock itself. No elastic anisotropy was found in the present analysis for aluminum.

¹⁵F. D. Murnaghan, *Proc. Nat. Acad. Sci. U.S.A.* **30**, 244 (1944).